

Orientational Order and Depinning of the Disordered Electron Solid

Min-Chul Cha and H. A. Fertig

Department of Physics and Astronomy and Center for Computational Sciences, University of Kentucky, Lexington, KY 40506
(June 17, 2021)

We study the ground state of two-dimensional classical electron solids under the influence of modulation-doped impurities by using a simulated annealing molecular dynamics method. By changing the setback distance as a parameter, we find that in the strong disorder limit the ground state configuration contains both isolated dislocations and disclinations, whereas in the weak disorder regime only dislocations are present. We show, via continuum elasticity theory, that the ground state of the lattice should be unstable against a proliferation of free disclinations above a critical dislocation density. Associated with this, the behavior of the threshold electric field as a function of the setback distance changes.

73.40.-c,73.50.Yg,74.60.Ge

Since Wigner [1] proposed a solid phase of electrons, searches for a Wigner crystal (WC) have been pursued in various systems. In a low density region, a realization of the WC on a helium film has been established [2]. The WC is also expected to be formed in two-dimensional systems in very strong magnetic fields [3]. Recently a considerable amount of experimental study has focused on the search for this magnetically induced WC [4,5]. All of these observations have been interpreted as indirect indications of a pinned WC. There is also some evidence of experimental observation of the WC at zero magnetic field in Si MOSFET [6]. However, disorder, which is ubiquitous, makes it difficult to interpret the experimental observations. For example, the value of the depinning threshold electric field of the presumed magnetically induced WC for slightly different sample geometries differs up two orders of magnitude [4]. To interpret experimental observations, therefore, it is necessary to understand the pinning sources and estimate the pinning forces. One aspect of this problem is that random impurities pin a WC and at the same time deform it, introducing defects in the lattice. Only a few studies have been devoted to clarify the possible sources of pinning [7] in the two dimensional electron system confined in a heterojunction. Furthermore, the details of the relation between the defects generated by impurities and the pinning [8] are not well understood.

In this paper, we study pinning and orientational order in a model of the classical two-dimensional electron system. Our calculations are most directly applicable to electrons on a helium film [9], although some of our basic conclusions should apply to heterojunction systems in strong magnetic fields, where the filling factor is quite

small, so that quantum exchange effects are unimportant [10]. Disorder is introduced by modulation-doped donors randomly located on a plane separated by a setback distance d from the two-dimensional electron plane. Since the charged electrons and ions are interacting by a $1/r$ potential, the effect of impurities is characterized by a dimensionless constant d/a_0 , where a_0 is the lattice constant of a perfect lattice. It is known that arbitrarily weak disorder destroys long-range translational order in two dimensions associated with a crystal lattice [11]. However, we can study the *orientational* order of this system, and the associated change in behavior of the depinning threshold electric field. From numerical simulations with up to 3200 particles, we have observed defects—predominantly dislocations and disclinations—generated by the impurity potential. In the weak disorder limit (large d/a_0), the ground state configuration contains a quasi-long range orientational order [12] (*i.e.* hexatic phase), and we observed no free disclinations in the system. However, as disorder increases, isolated disclinations appear, destroying the quasi-long range orientational order [13]. We will argue below, based on continuum elasticity theory, that above a threshold density of dislocations, it is always energetically favorable to create isolated disclinations.

Our principal results are summarized in Figs. 1 and 2. Fig. 1 shows the orientational correlation functions for different values of d/a_0 . One sees that the quasi-long range orientational order is destroyed in the strong disorder limit. Associated with this crossover, the behavior of the threshold electric field is changed as shown in Fig. 2. The crossover takes place approximately at $d/a_0 \approx 1.15 \pm 0.1$, which is consistent with the vanishing of orientational order. To qualitatively understand this behavior, it is necessary to observe the motion of the electrons as they depin. (Details will be published elsewhere [14].) We find that the electrons tend to flow along directions of the local bond orientation; *i.e.*, to flow along local symmetry directions of the crystal. Since the system does not have long range orientational order, it is necessary for electron to pass through regions of great strain in the lattice, where the orientation changes. These regions of strain represent bottlenecks in the electron flow. As the disorder strength is tuned and orientational order changes from quasi-long range to short range, the number of bottlenecks proliferates and there is a sharp increase in the threshold field. We also note that the threshold electric field is very sensitive to the setback distance, which might explain the very disparate values of this quantity

arXiv:cond-mat/9402021v1 4 Feb 1994

in experiments [4].

More explicitly, we study a system whose energy is given by

$$E = \sum_{i \neq j} \frac{e^2}{\epsilon |\vec{r}_i - \vec{r}_j|} - \sum_{ij} \frac{e^2}{\epsilon (|\vec{r}_i - \vec{R}_j|^2 + d^2)^{1/2}} \quad (1)$$

where $\{\vec{r}_i\}$ are the electron configurations, $\{\vec{R}_i\}$ are quenched donor configurations on a modulation-doped plane, d is the setback distance, and ϵ is a dielectric constant. Numerically, we use a simulated annealing molecular dynamics method [15] to find an electron configuration, $\{\vec{r}_i\}$, that corresponds to the ground state or, at least, a typical low energy metastable state. We impose periodic boundary conditions, and use the Ewald sum technique [16] to handle the long range interaction in computing energies and forces. Because our study focuses in part on the depinning properties of this system, and it is possible that the depinning will be inhomogeneous (*i.e.*, that current paths form inside the crystal), we must account for the fact that electrons exiting the system will need to reenter it on the opposite side of the unit cell. To minimize any mismatch of current patterns at the boundaries, along the direction of the depinning field we juxtapose two square boxes whose impurity configurations are mirror-images of each other.

We take $\epsilon = 13$ in the numerical simulations, and slowly lower the temperature from above the melting transition down to 20mK for a typical electron density $n = 5.7 \times 10^{10} \text{cm}^{-2}$. At this temperature we measure the orientational correlation functions, which are summarized in Fig. 1. The correlation functions can be well fitted by exponential forms in the strong disorder limit (small d). We find that the correlation length ξ is a slowly varying function for $d/a_0 < 1$; in the interval $1.1 < d/a_0 < 1.2$, the correlation length rises rapidly, suggesting a possible divergence (and an associated phase transition). However, once the correlation length exceeds our system size, fits to either an exponential form or a power law become possible, and it becomes difficult to precisely identify what value of d/a_0 would be the critical one in an infinite system. However, based on the sharp increase in $\xi(d)$, we suspect that it is in the vicinity of 1.2. This estimate is also consistent with the observation of the structure factor in Fig. 3, where the six-fold symmetry of the orientational order [12] appears only for the samples with setback distance bigger than 1.1.

We also measure the threshold depinning field. To do this, we shift the positions of the particles along a chosen direction by steps of $0.01a_0$ [15] up to 1–3 lattice constants. After each shift 200 MD steps are taken to equilibrate the system, and the pinning force is obtained in the next 100 MD steps from the averaging the force on particles due to impurities. The threshold field is determined by the maximum value of the pinning force multiplied by the dielectric constant during the shifting

process; error bounds may be obtained by comparing the heights of the several peaks that one sees. The results are shown in Fig. 2. We take two samples for each setback distance. We also determine the threshold field for several samples by gradually increasing an external field and by identifying the point at which the currents start to flow. The results obtained through the two methods are in good agreement. The behavior of the threshold depinning force changes around $d/a_0 = 1.15 \pm 0.1$, which suggest that disclinations produce extra pinning of the lattice.

We now describe how free disclinations might be favored in strongly disordered samples using standard elasticity theory [18]. Since the charged system requires charge neutrality at long wavelengths, we consider a model whose elastic energy is given by

$$\tilde{E} = \frac{1}{2} \int d^2\vec{r} [2\mu u_{ij}^2 + \lambda(\nabla \cdot \vec{u} - \delta\rho(\vec{r}))^2], \quad (2)$$

where μ and λ are Lamé coefficients, $\vec{u}(\vec{r})$ are displacement vectors, $u_{ij} = (1/2)(\partial u_i/\partial x_j + \partial u_j/\partial x_i)$, and $\rho(\vec{r}) = \rho_0 + a_0^{-2}\delta\rho(\vec{r})$ is an effective in-plane impurity density. (Summation convention is assumed for repeated indices.) Since the longitudinal sound velocity goes to infinity for $1/r$ interaction, we take the limit $\lambda \rightarrow \infty$ at the end of our calculation. This will guarantee that the electron density tracks the neutralizing background, which is the correct physics at long wavelengths. With defining a stress tensor

$$\Pi_{ij} = 2\mu u_{ij} + \lambda\delta_{ij}(\nabla \cdot \vec{u}), \quad (3)$$

we can divide Eq. (2) into the contributions from smooth elastic displacements and displacements related to defects which involve singularities.

$$\tilde{E} = E_0 + E', \quad (4a)$$

$$E_0 = \frac{\lambda}{2} \int d^2\vec{r} \delta\rho[\delta\rho - \nabla \cdot \vec{u}^0] \\ = \frac{\lambda}{2} \int d^2\vec{r} (\delta\rho)^2 [1 - \frac{\lambda}{2\mu + \lambda}] \rightarrow \mu \int d^2\vec{r} (\delta\rho)^2, \quad (4b)$$

$$E' = \frac{1}{2} \int d^2\vec{r} [\Pi'_{ij} u'_{ij} - \lambda(\nabla \cdot \vec{u}')\delta\rho], \quad (4c)$$

where \vec{u}^0 and \vec{u}' represent the regular and the singular parts, respectively, etc. We note that all these quantities are well-behaved as $\lambda \rightarrow \infty$. As with many crystal systems in the presence of disorder [8,17], we find that our electron crystal is unstable against the formation of highly separated dislocations even in the weak disorder limits [14], and this is certainly the case in our simulations. As the disorder strength is increased, the density of dislocations increases. It is instructive to consider the energy of a single disclination in a complexion of dislocations. We write the defect energy as

$$E' = E'_D + E'_{BD} + E'_{D\rho}, \quad (5)$$

where E'_D , E'_{BD} , and $E'_{D\rho}$ are energy of the disclination, the coupling energy between disclination and dislocations, and energy of interaction of the disclination directly with the background impurities, respectively. In a finite size system with area A , we have

$$E'_D = \frac{\mu}{72}A, \quad (6a)$$

$$E'_{BD} = s \frac{\mu\pi}{9} \sum_j (\vec{b}_j \times \vec{r}_j) \cdot \hat{z} \ln\left(\frac{\pi|\vec{r}_j|^2}{A}\right), \quad (6b)$$

where \vec{b}_j and \vec{r}_j are Burger's vectors and the position vectors of the dislocations, and $s = \pm 1$ is the "charge" of the disclination, specifying whether it is a 5-fold or 7-fold defect [13]. The contribution of $\langle E'_{D\rho} \rangle$, where $\langle \dots \rangle$ denotes a disorder average, scales only as $\sqrt{A \ln A}$, and so is negligible for large system sizes. We note that s may always be chosen such that $E'_{BD} < 0$ for any complexion of dislocations. The contribution E'_{BD} may be estimated by computing the average over complexions of disclinations. Assuming for simplicity that the dislocations are completely uncorrelated, $\langle \vec{b}(\vec{r}) \cdot \vec{b}(\vec{r}') \rangle \equiv \langle |\vec{b}| \rangle^2 \delta(\vec{r} - \vec{r}')$, we find

$$\langle E'_{BD} \rangle \approx -\sqrt{\langle |E'_{BD}|^2 \rangle} = -\frac{\langle |\vec{b}| \rangle \sqrt{\pi}}{36a_0} \mu A. \quad (7)$$

Thus, the net energy of an isolated disclination for large A is

$$E' \approx \left[\frac{1}{72} - \frac{\langle |\vec{b}| \rangle \sqrt{\pi}}{36a_0} \right] \mu A, \quad (8)$$

so it is energetically favorable on average to create a disclination if

$$\langle |\vec{b}| \rangle > \frac{1}{2\sqrt{\pi}} a_0. \quad (9)$$

Interpreting $\langle |\vec{b}| \rangle^2$ as the density of dislocations in lattice units, we estimate the critical density of dislocations as $n_b \approx (1/4\pi)a_0^{-2}$ above which disclinations are energetically favorable. This value is roughly in agreement with what we observe in our simulations, in which isolated disclinations appear when $n_b^{-1} \approx 17\text{--}22 a_0^2$. We note, finally, that our computation of $\langle E' \rangle$ essentially estimates the mean value of the disclination energy, if we computed the distribution of E' for all possible disclination locations. This mean scales to $\pm\infty$ as $A \propto N_b \rightarrow \infty$, where N_b is the number of dislocations. One can show that for a simple Gaussian distribution of $\vec{b}(\vec{r})$, the variance of $\langle E' \rangle$ is also proportional to N_b , so that this model predicts a crossover behavior from a state with very few disclinations to one with many at the critical dislocation density. It is interesting to speculate that a more realistic distribution for $\vec{b}(\vec{r})$ could convert this crossover to a true phase transition. This would be quite consistent with our simulations, where isolated disclinations are

observed for small d/a_0 , and there is an apparently diverging orientational correlation length just before they disappear. Details of this calculation will be presented elsewhere [14].

In conclusion, we have observed a crossover between a weak disorder regime and a strong disorder regime in a study of a model Wigner crystal under the influence of the modulation-doped donor impurities as we tune the setback distance. In the weak disorder regime, we have a hexatic phase where a quasi-long range orientational order is present, whereas in the strong disorder regime isolated disclinations destroy the orientational order. The crossover places $d/a_0 = 1.15 \pm 0.1$. Associated with this crossover, the behavior of the threshold electric field changes. We argue by a continuum elasticity theory that this crossover can be understood as a proliferation of disclinations when the density of dislocations is bigger than a certain critical value.

ACKNOWLEDGMENTS

MCC is grateful for helpful discussions with S. M. Girvin and a computational assistance of Clayton Heller. This work was supported in part by NSF DMR 92-02255.

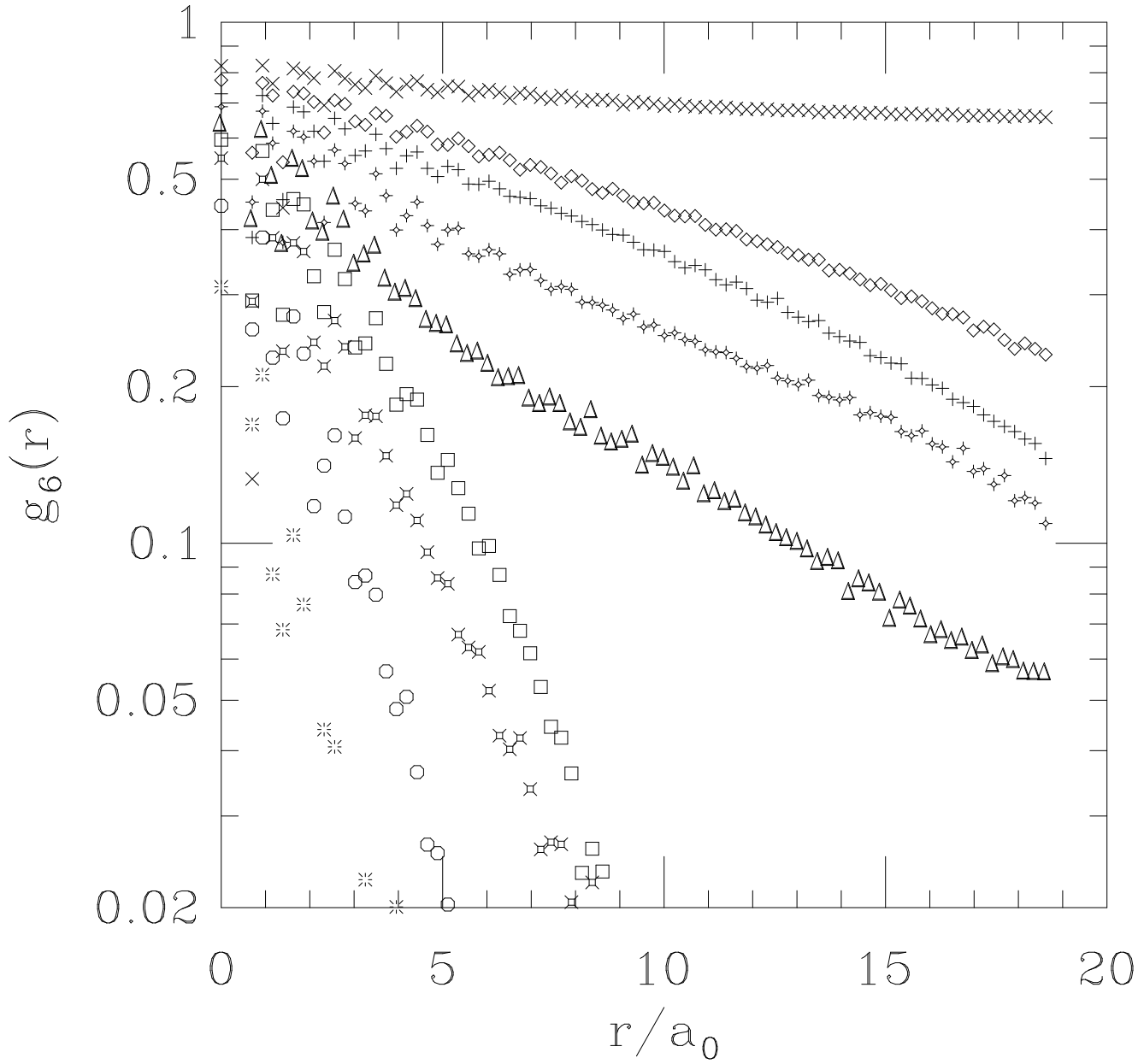
-
- [1] E. Wigner, *Phys. Rev.* **46**, 1002 (1934).
 - [2] C. C. Grimes and G. Adams, *Phys. Rev. Lett.* **42**, 795 (1979).
 - [3] Y. E. Lozovik and V. I. Yudson, *Pis'ma Zh. Eksp. Teor. Fiz.* **22**, 26 (1975) [*JETP Lett.* **22**, 11 (1975)]; Pui K. Lam and S. M. Girvin, *Phys. Rev. B* **30**, 473 (1984); D. Levesque, J. J. Weis, and A. H. MacDonald, *Phys. Rev. B* **30**, 1056 (1984).
 - [4] V. J. Goldman, M. Santos, M. Shayegan, and J. E. Cunningham, *Phys. Rev. Lett.* **65**, 2189 (1990); F. I. B. Williams, P. A. Wright, R. G. Clark, E. Y. Andrei, G. Deville, D. C. Glattli, O. Probst, B. Etienne, C. Dorin, C. T. Foxon, and J. J. Harris, *Phys. Rev. Lett.* **66**, 3285 (1991); H. W. Jiang, H. L. Stormer, D. C. Tsui, L. N. Pfeiffer, and K. W. West, *Phys. Rev. B* **44**, 8107 (1991).
 - [5] H. W. Jiang, R. L. Willett, H. L. Stormer, D. C. Tsui, L. N. Pfeiffer, and K. W. West, *Phys. Rev. Lett.* **65**, 633 (1990); Yuan P. Li, T. Sajoto, L. W. Engel, D. C. Tsui, and M. Shayegan, *Phys. Rev. Lett.* **67**, 1630 (1991); H. Buhmann, W. Joss, K. v. Klitzing, I. V. Kukushkin, A. S. Plaut, G. Martinez, K. Ploog, and V. B. Timofeev, *Phys. Rev. Lett.* **66**, 926 (1991); E. Y. Andrei, G. Deville, D. C. Glattli, F. I. B. Williams, E. Paris, and B. Etienne, *Phys. Rev. Lett.* **60**, 2765 (1988); H. L. Stormer and R. L. Willett, *Phys. Rev. Lett.* **62**, 972 (1989); M. A. Paalanen, R. L. Willett, P. B. Littlewood, R. R. Ruel, K. W. West,

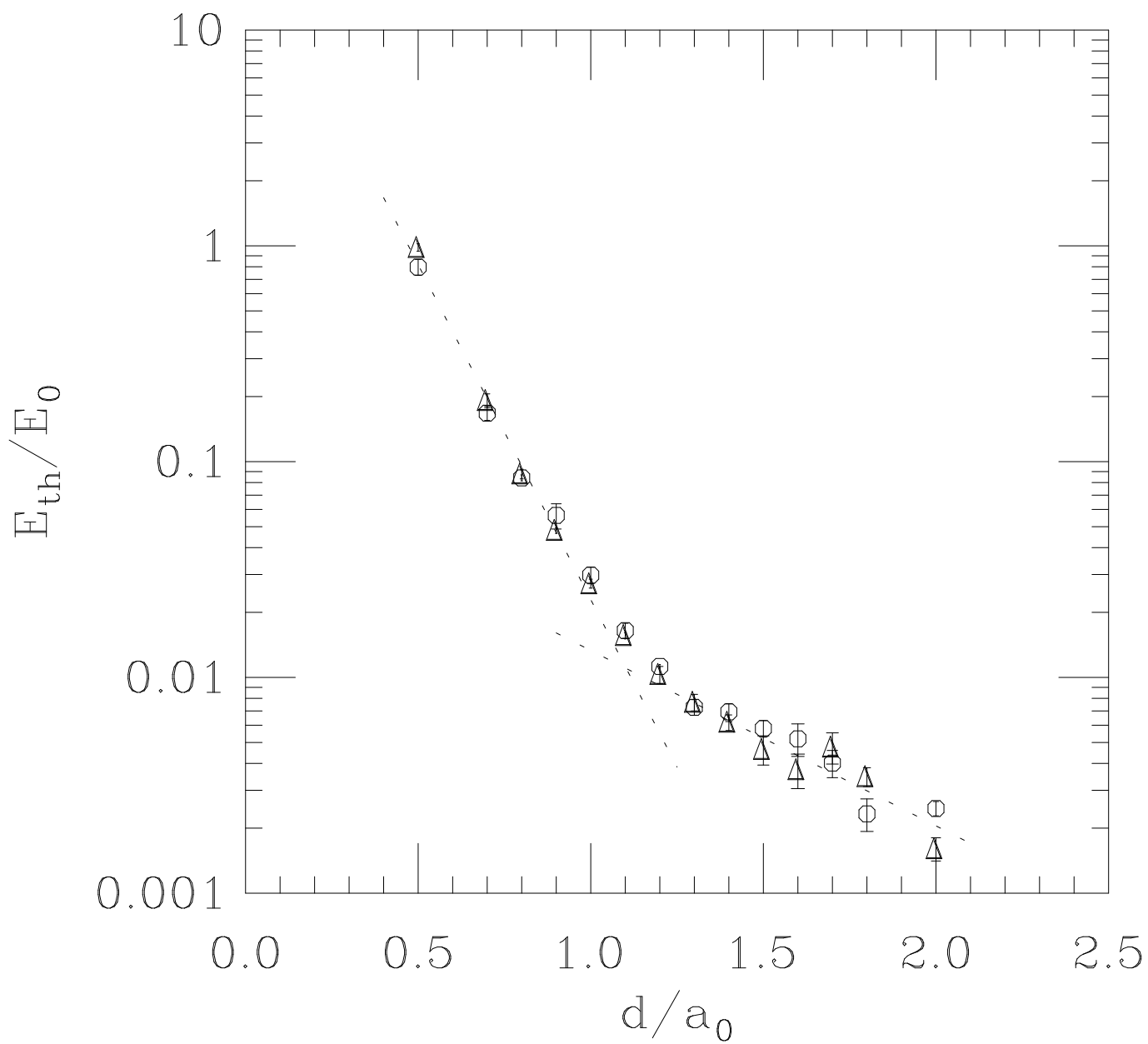
- L. N. Pfeuffer, and D. J. Bishop, *Phys. Rev. B* **45**, 11342 (1992).
- [6] V. M. Pudalov, M. D'Iorio, S. V. Kravchenko, and J. W. Campbell, *Phys. Rev. Lett.* **70**, 1866 (1993); S. V. Kravchenko, Jos A. A. J. Perenboom, and V. M. Pudalov, *Phys. Rev. B* **44**, 13513 (1991).
- [7] I. M. Ruzin, S. Marianer, and B. I. Shklovskii, *Phys. Rev. B* **46**, 3999 (1992); B. G. Normand, P. B. Littlewood, and A. J. Millis, *Phys. Rev. B* **46**, 3920 (1992).
- [8] A.-C. Shi and A. J. Berlinsky, *Phys. Rev. Lett.* **67**, 1926 (1991).
- [9] H.-W. Jiang and A. J. Dahm, *Phys. Rev. Lett.* **62**, 1396 (1989).
- [10] Kazumi Maki and Xenophon Zotos, *Phys. Rev. B* **28**, 4349 (1983).
- [11] Y. Imry and S.-k. Ma, *Phys. Rev. Lett* **35**, 1399 (1975); D. J. Bergman, T. M. Rice, and P. A. Lee, *Phys. Rev. B* **15**, 1706 (1977).
- [12] D. R. Nelson, M. Rubinstein, and F. Spaepen, *Philos. Mag. A* **46**, 105 (1982).
- [13] D. R. Nelson and B. I. Halperin, *Phys. Rev. B* **19**, 2457 (1979); D. R. Nelson, *Phys. Rev. B* **26**, 269 (1982).
- [14] Min-Chul Cha and H. A. Fertig, (unpublished).
- [15] A. Brass, H. J. Jensen, and A. J. Berlinsky, *Phys. Rev. B* **39**, 102 (1989); H. J. Jensen, A. Brass, and A. J. Berlinsky, *Phys. Rev. Lett.* **60**, 1676 (1988).
- [16] L. Bonsall and A. A. Maradudin, *Phys. Rev. B* **15**, 1959 (1977); D. S. Fisher, B. I. Halperin, and R. Morf, *Phys. Rev. B* **20**, 4692 (1979)
- [17] S. N. Coppersmith, *Phys. Rev. Lett.* **65**, 1044 (1990).
- [18] L. D. Landau and E. M. Lifshitz, *Theory of Elasticity* (Pergamon, New York, 1986).

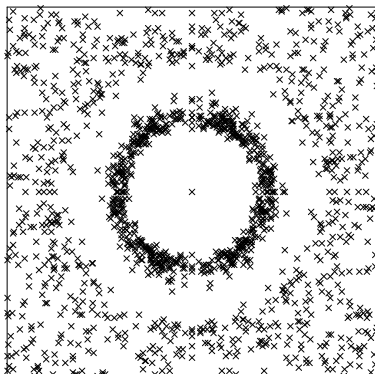
FIG. 1. The orientational correlation functions for various setback distances. Different symbols represent data for samples with different setback distance. From top to bottom, $d/a_0 = 2.0, 1.7, 1.5, 1.3, 1.2, 1.1, 1.0, 0.9$, and 0.8 .

FIG. 2. The depinning threshold field observed in various samples in the unit of $E_0 = e/(\epsilon a_0^2)$. The dotted lines are guides to the eye.

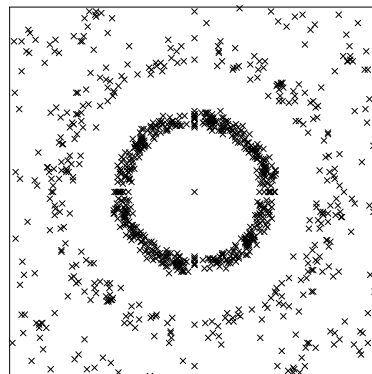
FIG. 3. The magnitude of the structure factor, $|S(\vec{G})|$, in the reciprocal lattice vector space for samples with $d/a_0 =$ (a)0.8, (b)1.0, (c)1.1, (d)1.2, (e)1.4, and (f)1.7. Only the points at which $|S(\vec{G})| > \frac{1}{2}|S(\vec{G})|_{\max}$ are plotted. For large setback distances, a six-fold symmetry appears, indicating the presence of the quasi-long range orientational order.



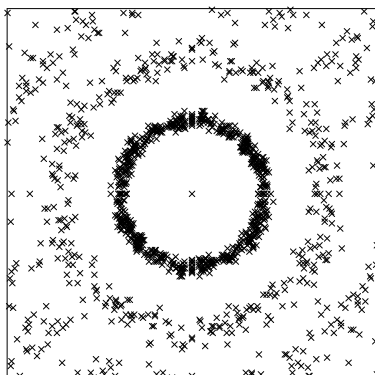




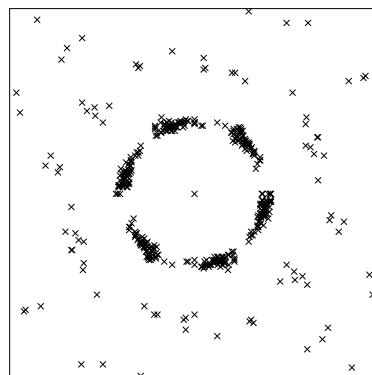
(a)



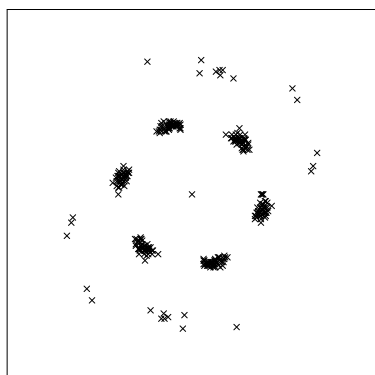
(b)



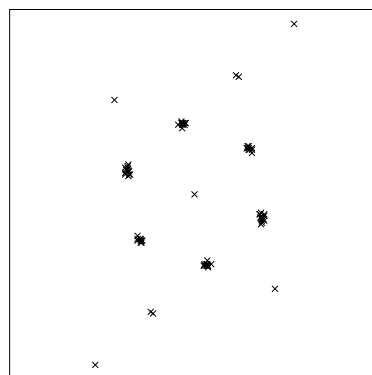
(c)



(d)



(e)



(f)